Electrochemistry and Electrogenerated Chemiluminescence of *n*-Pentyl and Phenyl BODIPY Species: Formation of Aggregates from the Radical Ion Annihilation Reaction

Alexander B. Nepomnyashchii,[†] Martin Bröring,[‡] Johannes Ahrens,[‡] Robin Krüger,[‡] and Allen J. Bard*[,†]

Center for Electrochemistry, Chemistry and Biochemistry Department, The University of Texas at Austin, Austin, Texas 78712, Institut für Anorganische und Analytische Chemie, Technische Universität Carolo-Wilhelmina, Hagenring 30, 38106 Braunschweig, Germany

Received: June 9, 2010; Revised Manuscript Received: July 22, 2010

The electrochemistry and the electrogenerated chemiluminescence (ECL) of the BODIPY species (2,6-diethyl-1,3,5,7-tetramethyl-8-*n*-pentyl-4,4-difluoro-4-bora-3a,4a-diaza-*s*-indacene, i.e., B^8-*n*-pentyl), an aromatic monomer (B^8-phenyl), and a closely related dimer were examined. The B^8-*n*-pentyl species with the *n*-pentyl donor chain in the meso position shows good electrochemical behavior in MeCN with the formation of stable radical ions. The ECL emission is characterized by long-wavelength emission during consecutive oxidation and reduction steps. This is attributed to aggregate formation on radical ion annihilation, the extent of which increased with increasing concentration of the compound. The B^8-phenyl electrochemistry also shows stable radical ions. However, B^8-phenyl with the meso phenyl group ECL emission does not show any long-wavelength emission. The synthesized dimer closely related to this species shows two electrochemical oxidations with peak separations of 0.5 V and two reductions with peak separations 0.2 V, which corresponds to a high degree of intermolecular interactions in the molecule. The growth of additional electrochemical peaks during the oxidation and reduction of B^8-*n*-pentyl was not seen, and both radical ions were stable, suggesting that emitting secondary products were not formed.

1. Introduction

This research is concerned with the electrochemical behavior and electrogenerated chemiluminescence (ECL) of the boron dipyrromethene (BODIPY) dyes (Scheme 1).[1] The electrochemical and ECL properties of boron dipyrromethene (BODIPY) compounds are of interest because they often show clean voltammetry in aprotic solvents and excellent stability of oxidation and reduction products and are efficient, tunable emitters, hence making them excellent candidates for ECL applications. The BODIPY compounds also show good stability and high solubility in polar solvents. BODIPY compounds have found application as labels in biological studies, in optical devices, and as laser dyes.[1−5] They can show very high fluorescence efficiencies (often close to 1), and their spectra may be easily tuned over a wide wavelength range. They can also be labeled with different groups for sensing applications.[6−8] Several electrochemical and ECL studies of the BODIPY dyes have been reported.[9−14] Good electrochemical stability of the electrogenerated radical ions and good ECL efficiency require substitution of reactive positions 1−3 and 5−8.[9,11] This is very different from fluorescence where a higher efficiency is found for the less substituted dyes.[1,9] The potential for oxidation and reduction depends on the nature of the substituent donor or acceptor groups in different positions. In a recent study of a meso-amide-substituted BODIPY (B^8-amide) dye, where ECL was generated by chronoamperometric stepping to the oxidative and reductive potentials of the dye, complicated behavior was observed.[10] The electrochemistry was characterized by reversible electron transfer for both reduction and oxidation, but the ECL emission showed a distinct peak at longer wavelengths than seen in photoluminescence (PL) and the observed emission on repeated pulsing was anomalous. The reason for these effects was not clear, although there was some evidence for the formation of J aggregates, excimers or films on the electrode surface. There was also the possibility of a reaction following electron transfer with the formation of a dimer or another electrochemical product.

SCHEME 1: Schematic Representation of the BODIPY Skeleton

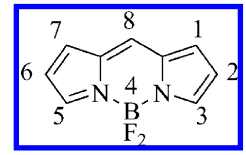

In this study, we investigated the nature of the long-wavelength emission found with BODIPY dyes for a B^8-*n*-pentyl dye (Scheme 2a) where the long amide chain in the meso 8 position B^8-amide of the earlier study[10] is replaced by an *n*-pentyl group. The electrochemistry and ECL of this dye were studied along with the effect of intra- and intermolecular interactions on the ECL stability. We also investigated the fluorescence, voltammetric, and ECL behavior of the B^8-phenyl monomer and its related dimer (Scheme 2b,c) and compare the behavior to that of the B^8-*n*-pentyl species.

ECL is a powerful tool for elucidating the properties of organic molecules[15] and has been used for biosensing, which could lead to application of BODIPY-based labels. The various mechanisms of ECL processes have been extensively discussed.[15] One method that is found in aprotic media is radical ion annihilation:

[†] The University of Texas at Austin.
[‡] Technische Universität Carolo-Wilhelmina.

10.1021/jp105312j
Published on Web 08/11/2010

$$A + e \rightarrow A^{\bullet -} \quad (1)$$

$$A - e \rightarrow A^{\bullet +} \quad (2)$$

$$A^{\bullet -} + A^{\bullet +} \rightarrow {}^1A^* + A \quad (3)$$

$$A^{\bullet -} + A^{\bullet +} \rightarrow {}^3A^* + A \quad (4)$$

$${}^3A^* + {}^3A^* \rightarrow {}^1A^* + A \quad (5)$$

$${}^1A^* \rightarrow A + h\nu \quad (6)$$

An alternative involves a co-reactant, which can serve to generate a useful reductant on oxidation (or oxidant on reduction) to react with the emission precursor. For example, tri-*n*-propylamine (TPrA) is widely used commercially in aqueous systems for immunochemistry.[16,17] The mechanism of its action can be presented as

$$A - e^- \rightarrow A^{\bullet +} \quad (7)$$

$$TPrA - e^- \rightarrow TPrA^{\bullet +} \quad (8)$$

$$TPrA^{\bullet +} \rightarrow TPrA^{\bullet} + H^+ \quad (9)$$

$$A^{\bullet +} + TPrA^{\bullet} \rightarrow {}^1A^* + TPrA^+ \quad (10)$$

$${}^1A^* \rightarrow A + h\nu \quad (11)$$

Reductive coreactants (e.g., benzoyl peroxide (BPO), $S_2O_8^{2-}$) can also be used.[18−21] For example, the mechanism of the BPO-based system can be presented as

$$A + e \rightarrow A^{\bullet -} \quad (12)$$

SCHEME 2: Structures of (a) B[8]-*n*-pentyl, (b) B[8]-phenyl, and (c) a Dimer

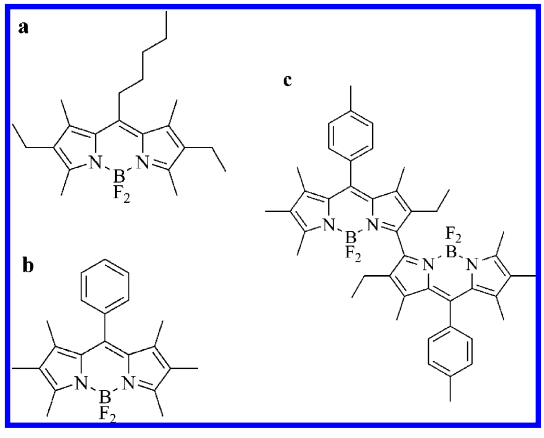

$$A^{\bullet -} + BPO \rightarrow A + BPO^{\bullet -} \quad (13)$$

$$BPO^{\bullet -} \rightarrow C_6H_5CO_2^- + C_6H_5CO_2^{\bullet} \quad (14)$$

$$A^{\bullet -} + C_6H_5CO_2^{\bullet} \rightarrow {}^1A^* + C_6H_5CO_2^- \quad (15)$$

Co-reactants can often be used to help elucidate ECL reaction mechanisms by contrasting the behavior with annihilation ECL.[15]

2. Experimental Section

2.1. Chemicals. B[8]-*n*-pentyl was purchased from Exciton Inc. (St. Louis, MO) (catalog number PM 567A). The B[8]-phenyl BODIPY monomer and dimer were synthesized according to the procedures previously reported.[22] Electrochemical-grade anhydrous MeCN (99.93%), dichloromethane (DCM) (99.8%), and 99% tri-*n*-propylamine were from Aldrich Chemical Co. (Milwaukee, WI) and used without further purification. Electrochemical-grade supporting electrolyte tetra-*n*-butyl-ammonium hexafluorophosphate ($TBAPF_6$) and benzoyl peroxide (BPO) were from Fluka.

2.2. Apparatus and Methods. UV−vis and fluorescence measurements were performed for B[8]-*n*-pentyl in MeCN and for B[8]-phenyl and the dimer in DCM. The quantum yield was determined and compared with the literature results using fluorescein as a standard. Absorbance measurements were obtained using a DU 640 spectrophotometer (Beckman, Fullerton, CA); a 1 cm quartz cuvette was used in all measurements. Fluorescence measurements were carried out with a double-beam QuantaMaster Spectrofluorimeter (Photon Technology International, Birmingham, NJ). A 70 W Xe lamp was used as the light source, and the slit width was 0.5 mm. Fluorescence concentration measurements were made using a UV lamp as an excitation source and a Princeton Instruments Spec-10 CCD camera (Trenton, NJ) with an Acton SpectraPr-150 monochromator (Acton, MA) as a detector. The CCD wavelengths were calibrated with a Hg/AR pen-ray lamp from Oriel (Stratford, CT). Electrochemical experiments were done under anhydrous oxygen-free conditions. Solutions were prepared in a helium-atmosphere drybox (Vacuum Atmospheres Corp., Hawthorne, CA) or in an argon-atmosphere drybox (UniLab 2000, M. Braun Inc., Stratham, NH). After preparation, the solution was sealed with a Teflon cap. A 0.0314 cm^2 Pt working electrode was used for the cyclic voltammetry experiments, and a J-type Pt electrode with the same area was used for the ECL experiments with the CCD. The geometric electrode area was determined by chronoamperometry with a 2 mM solution of ferrocene in MeCN assuming a diffusion coefficient, D, of 1.2×10^{-5} cm^2/s. The D values of the dyes were determined by the scan rate dependences from the Randles−Ševčik equation and chronoamperometric pulsing for 1 s and using the Cottrell equation. The working electrode was polished after each experiment with 0.3 μm alumina (Buehler, Ltd., Lake Bluff, IL), sonicated in ethanol and in water for 5 min, and dried in the oven at 120 °C. An Ag wire was used as a quasi-reference electrode (QRE), and Pt wire was used as a counter electrode. The potential of the QRE was calibrated using ferrocene as a standard that has $E^{o\prime} = 0.342$ V vs SCE.[10] Cyclic voltammetry and chronoamperometry measurements were carried out with CHI 660 and CHI 660D electrochemical workstations (CH Instruments, Austin, TX). ECL spectra were

obtained by using either the CHI 660 or an Eco Chemie Autolab PGSTAT30 potentiostat (Utrecht, The Netherlands). ECL spectra for the annihilation of B^8-*n*-pentyl and B^8-phenyl were recorded by potential pulsing with a pulse width of 0.1 s for potentials of 80 mV beyond the peak potentials for 1 min. ECL measurements for the dimer was made from around 80 mV after the first peak. The slit width was set to be 5 mm for all ECL measurements except for the TPrA measurement where it was set at 1 mm. The spectra were collected by a Princeton Instruments Spec-10 CCD camera with an Acton SpectraPr-150 monochromator. ECL intensity−time curves were obtained by recording the total emission with a photomultiplier tube (PMT, Hamamatsu R4220, Japan). A Kepco high-voltage power supply operated at a standard voltage of −750 V was applied to the PMT. An electrometer (model 6517, Keithley Instruments Inc., Cleveland, OH) was used to collect the ECL signal from the PMT. Experiments at 77 K were carried out using Spex Fluorolog 1 (Horiba Jobin Yvon, Tokyo, Japan) with Labview software, a 450 W sodium lamp and a 0.1 mm slit width with a cryostat (5T-100, Janis, Wilmington, MA) using liquid nitrogen and pumping during the experiment to avoid condensation. Digital simulations were done using Digisim software (Bioanalytical Systems, West Lafayette, IN).[23−26]

3. Results

3.1. Photophysical Studies. Absorption spectra of B^8-*n*-pentyl show the presence of the usual BODIPY S0−S1 transition in the visible wavelength range and the S0−S2 transition in the UV (Figure 1a, Table 1). Only one PL emission peak is observed over a concentration range of 10 μM to 5 mM (Figure 2). The quantum yield is 0.7 to 1 in MeCN, as is typical of many BODIPY dyes, with a relatively small Stokes shift.[1] The addition of alkyl groups to the meso position causes no substantial changes in the spectroscopic properties, so the fluorescence maxima of the B^8-*n*-pentyl dye and the B^8-amide are about the same.

No evidence of dimerization or aggregation (e.g., changes with concentration) was found by the fluorescence measurements. The PL properties of the aromatic BODIPY dimer and B^8-phenyl have been investigated previously.[22,27] B^8-phenyl in DCM showed the usual BODIPY absorption (Figure 1b, Table 1), and the dimer showed the excitonic splitting of the S0−S1 523 nm transition in the monomer to one at lower and the other at higher energy (Figure 1c). The fluorescence emission of the dimer shows a peak that is red shifted as compared to the monomer. Fluorescence studies showed no differences over a wide range of concentrations, suggesting the absence of intermolecular interactions. The B^8-phenyl and dimer showed the same location of the fluorescence emission in MeCN, DCM, ethanol, and acetone with a dependence on the fluorescence quantum yield on the solvent. *Es* in Table 1 stands for energy of fluorescence.

3.2. Electrochemical Studies. Electrochemical results for the studied dyes are summarized in Table 2.

The B^8-*n*-pentyl dye showed chemically reversible electrochemistry on both oxidation and reduction (Figure 3). The nernstian character of the electrochemical behavior of the dye was confirmed by digital simulation, where the theoretical and experimental results agreed well and are shown in the Supporting Information (Figure S1). Electrochemical studies of the B^8-phenyl in MeCN showed similar behavior to that of the B^8-*n*-pentyl, with some small reduction waves on a reverse scan following the oxidation; the dimer, however,

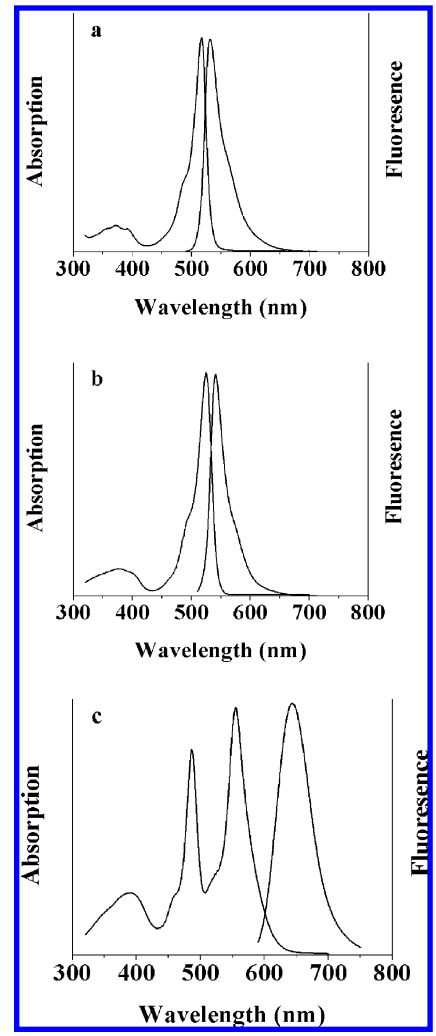

Figure 1. Absorption and fluorescence spectra of 2 μM BODIPY dyes: (a) B^8-*n*-pentyl in acetonitrile, (b) B^8-phenyl in DCM, and (c) dimer in DCM.

TABLE 1: Photophysical Properties of the Studied BODIPY Compounds

dye	λ_{max} (abs) (nm)	λ_{max} (fluor) (nm)	ε (10^4 M^{-1} cm^{-1})	Φ_{fluor}	*Es* (ev)
B^8-*n*-pentyl	372, 518	532	0.74, 8.80	0.8	2.33
B^8-phenyl	376, 523	541	0.70, 8.60	1.0	2.29
dimer	389, 486, 556	643	1.66, 6.44, 7.36	0.7	1.93

show a higher instability of the reduced and oxidized species, probably because of a reaction with trace impurities, probably water, in the MeCN (Figure 4). By changing the solvent from MeCN to DCM, more reversible and cleaner electrochemistry on both oxidation and reduction was seen, especially for the dimer. The electrochemistry of B^8-phenyl showed behavior similar to that of the B^8-*n*-pentyl dye with one-electron reduction and oxidation waves and very similar half-wave potential differences between oxidation and reduction processes (Figure 5). Digital simulations were also carried out and confirmed the presence of nernstian electrochemical oxidation and reduction waves (Supporting Information, Figure S2). The dimer possesses contrasting electrochemical behavior when compared to that of typical BODIPY monomers, showing two reversible reduction and oxidations waves, with a splitting between peaks of about 0.24 V for the reduction and 0.5 V for the oxidation (Figure 6). As will be

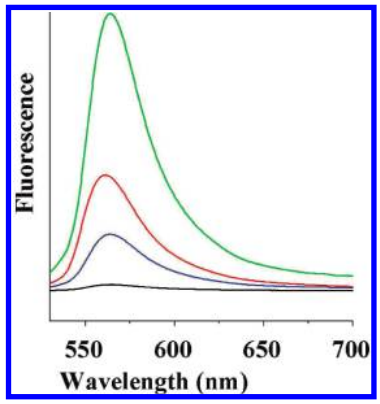

Figure 2. Fluorescence spectra for different concentrations of B^8-*n*-pentyl in acetonitrile: 0.01 mM (black line), 0.2 mM (blue line), 1 mM (red line), and 5 mM (green line).

TABLE 2: Electrochemical Studies of the BODIPY Compounds

dye	E_p (V vs SCE) A/A$^+$	E_p (V vs SCE) A/A$^-$	λ_{max} (ECL) (nm)	Φ_{ECL}	ΔH_s (eV)	D (cm^2/s)
B^8-*n*-pentyl	1.30	−1.21	540 669	0.18	2.30	6.1×10^{-6}
B^8-phenyl	1.01	−1.40	560	0.17	2.22	6.3×10^{-6}
dimer	0.97 1.47	−1.34 −1.59	666	0.10	2.17 2.85	5.0×10^{-6}

discussed in more detail elsewhere,[28] monomeric BODIPY species show unusually large splitting between the first and second reduction waves (~1 V). The much smaller splitting between these waves in the dimer suggests the consecutive addition or removal of electrons from the two BODIPY centers. The scan rate dependence for both the reduction and oxidation waves demonstrates chemically reversible behavior (Supporting Information, Figure S3). The diffusion coefficients determined for B^8-*n*-pentyl and B^8-phenyl are fairly similar and larger than for the larger aromatic dimer. Thus, this work confirms that BODIPY dyes completely substituted with alkyl or aryl groups show reversible electrochemistry, where the difference in the redox potentials is related to the substituent in the 8 position and the number of subunits. The nernstian behavior and high stability of substituted BODIPY compounds make them especially appropriate for the electrochemical study of intermolecular interactions.

3.3. Electrogenerated Chemiluminescence. The excited states for all of these compounds can be generated by electron transfer between the oxidized and reduced forms by electrochemical pulsing or scanning between the appropriate potentials. ECL spectra for B^8-*n*-pentyl show the presence of two peaks: one with the wavelength maximum close to that seen in fluorescence and one at a longer wavelength (Figure 7), just like the ECL behavior seen with the B^8amide.[10] The only difference is the size of the shift of the long-wavelength peaks: 190 nm for the B^8 amide versus 129 nm for B^8-*n*-pentyl. In both cases, there is a small shoulder that is also seen at an even longer wavelength. However when the excited state is generated with a co-reactant, either TPrA at oxidative potentials or BPO at reductive potentials, only a single ECL peak is observed that is very close to the fluorescence spectrum (Figure 7c). A slightly longer wavelength for the ECL first peak compared to the fluorescence peak obtained at much lower concentrations can be attributed to an inner filter effect as seen for PL experiments at high concentrations (e.g., where an apparent shift of the wavelength of the fluorescence is seen (Figure 2)). Thus, the excited state associated with the long-wavelength ECL peak (at ~670 nm) is favorably formed in the annihilation process. This effect of the lack of a second peak or broad, long wavelength emission in the presence of a co-reactant has been seen in other studies.[10,29] Studies with both co-reactants also exclude the possibility that a slight instability of either the radical anion or cation produces a product that emits at longer wavelength.

The ECL spectra of the B^8-phenyl and dimer show a single peak with a wavelength close to that in the fluorescence spectra for both compounds (Figure 8a,b). The ECL spectra for the B^8-phenyl and dimer were generated in both DCM and MeCN and show the same ECL maximum at a higher intensity with DCM compared to that with MeCN, probably because of stability issues and also the higher fluorescence quantum efficiency for DCM (Figure 8).[27] A comparison of the ECL spectra of B^8-*n*-pentyl and the B^8-phenyl at two different concentrations clearly shows that the relative size of the long-wavelength band, which is absent for B^8-phenyl, is strongly concentration-dependent (Figure 9).

The difference between the oxidation and reduction half-wave potentials allows one to determine the nature of the excited state formed on radical ion annihilation in ECL from the Gibbs equation for the ECL process: $\Delta G_{ann} = \Delta H_s - T\,\Delta S$.[15] The entropic factor is conventionally assumed to be about 0.1 eV under the usual experimental conditions. The emission energy from the spectra for B^8-*n*-pentyl is 2.27 eV, and that for B^8-phenyl is 2.20 eV, which is slightly smaller than the 2.30 and 2.22 eV calculated from the difference in the half-wave potentials. The closeness of these values makes the determina-

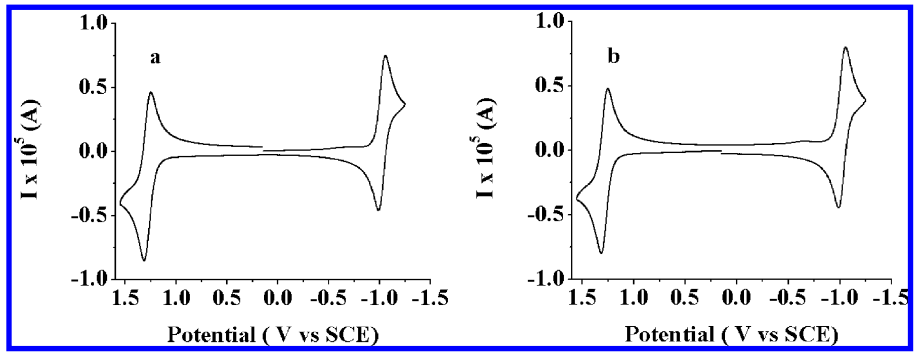

Figure 3. Cyclic voltammogram of 1.5 mM B^8-*n*-pentyl at a scan rate of 0.1 V/s in acetonitrile at a platinum working electrode (area = 0.0314 cm^2); supporting electrolyte, 0.1 M $TBAPF_6$. (a) Forward scan in the negative direction and (b) forward scan in the positive direction. As shown, the current scale encompasses ±10 μA.

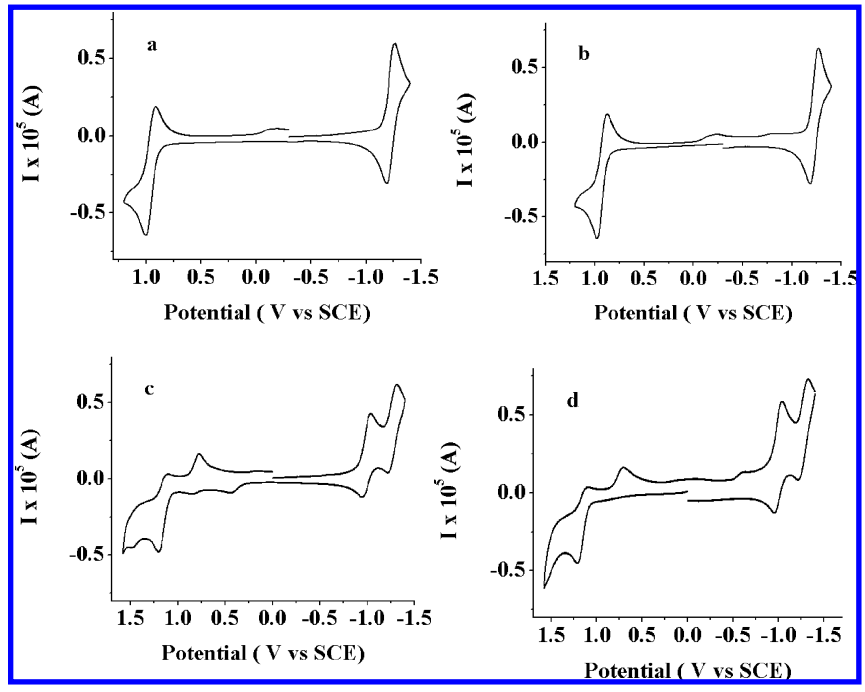

Figure 4. Cyclic voltammogram of (a, b) 1.0 mM B^8-phenyl and (c, d) a 1.4 mM dimer at a scan rate of 0.1 V/s in acetonitrile at a platinum working electrode (area = 0.0314 cm^2); supporting electrolyte, 0.1 M $TBAPF_6$. (a, c) Forward scan in the positive direction and (b, d) forward scan in the negative direction. As shown, the current scale encompasses ±5 μA.

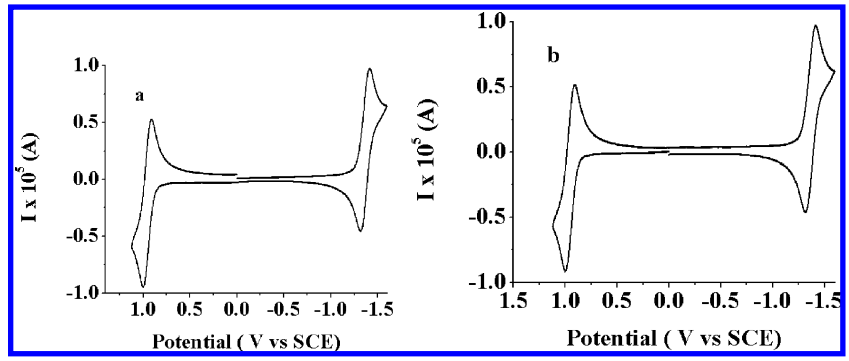

Figure 5. Cyclic voltammogram of 1.5 mM B^8-phenyl at a scan rate of 0.1 V/s in DCM at a platinum working electrode (area = 0.0314 cm^2); supporting electrolyte, 0.1 M $TBAPF_6$. (a) Forward scan in the negative direction and (b) forward scan in the positive direction. As shown, the current scale encompasses ±5 μA.

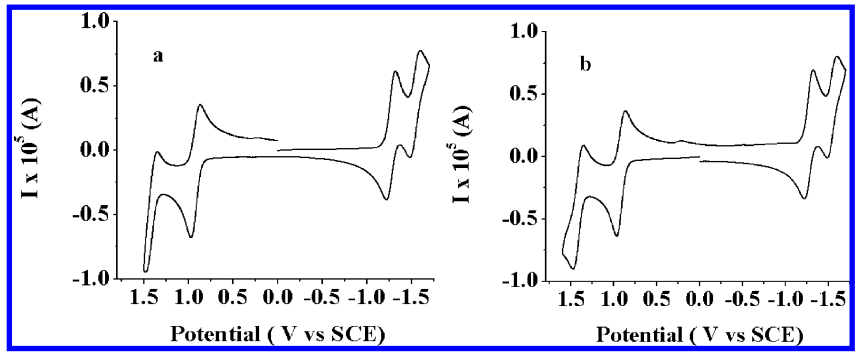

Figure 6. Cyclic voltammogram of a 1.4 mM dimer at a scan rate of 0.1 V/s in DCM at a platinum working electrode (area = 0.0314 cm^2); supporting electrolyte, 0.1 M $TBAPF_6$. (a) Forward scan in the negative direction and (b) forward scan in the positive direction. As shown, the current scale encompasses ±10 μA.

tion of the electron-transfer-formed excited state a little uncertain, but it can probably be best described as an ST route in which both singlets and triplets are formed. The dimer shows an energy of annihilation (2.17 eV) that is significantly larger than the 1.86 eV emission energy, so the singlet route for ECL probably dominates.

4. Discussion

An ongoing question that arises in many ECL studies where the annihilation reaction results in the occurrence of a second peak at longer wavelengths that is not seen in PL is the cause of such a peak. For example, in the annihilation ECL for B^8-*n*-pentyl, the peak could arise from an excimer or other

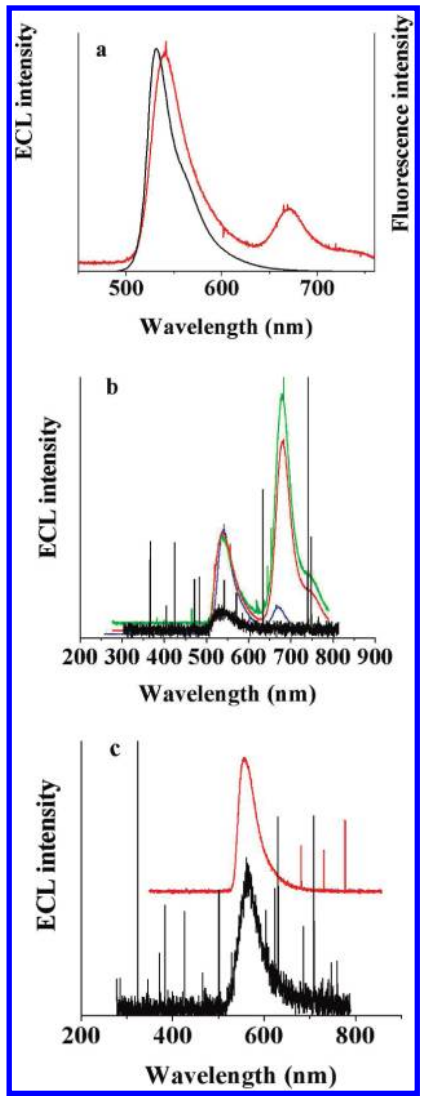

Figure 7. (a) ECL (red) and fluorescence (black) spectra for the B^8-*n*-pentyl dye in acetonitrile. The concentration of the B^8-*n*-pentyl for ECL measurements is 0.2 mM, and that for the fluorescence measurements is 2 μM. (b) ECL spectra for different concentrations of the B^8-*n*-pentyl: 0.01 mM (black line), 0.2 mM (blue line), 1 mM (red line), and 5 mM (green line). (c) ECL spectra for 1 mM B^8-*n*-pentyl in the presence of 50 mM TPrA (black line) and 50 mM BPO (red line). ECL spectra were generating by pulsing from −1.29 to 1.38 V for the annihilation process, from 0 to −1.29 V in the presence of BPO, and from 0 to 1.38 V for the TPrA case. A platinum working electrode with an area of 0.0314 cm^2 and 0.1 M $TBAPF_6$ were used for all measurements. A 10 Hz frequency of pulsing was used for all experiments. Stepping time, 1 min.

noncovalent aggregation of molecules, film formation, or dimerization or the production of other chemical species from reactions of the radical ions that emit at longer wavelengths. The current study provides evidence that aggregate formation may be responsible for the longer-wavelength ECL and not other effects. Film formation can be excluded because BODIPY films generally do not show high fluorescence efficiency in the absence of the bulky substituents.[30] The B^8-*n*-pentyl films show low fluorescence emission, but we were not able to generate stable ECL spectra. The formation of products from the reactions of the radical ions is also unlikely in this case because the CV behavior shows good stability of both the radical anion and cation. The formation of a covalent dimer is unlikely for the same reason, even though the spectrum is close to that seen with the B^8-phenyl dimer (Figure 9). The B^8-*n*-pentyl dye is completely substituted with simple alkyl chains, so there is no likely site for the formation of a covalent dimer, even on radical ion annihilation. Whereas the formation of an excimer on radical annihilation in ECL, as has been proposed in other studies, is a possibility because the intensity of the long-wavelength emission is essentially absent when the ECL is generated with co-reactants (either TPrA or BPO), the shape of the emission peak is too sharp compared to that seen for typical excimers. Generally, excimer emission is characterized by a very broad emission because there is no stable ground state of the emitting species.[31] The best explanation is that an aggregate of B^8-*n*-pentyl dye forms on radical annihilation.

Thus, the process proposed is

$$B^8\text{-}n\text{-pentyl} + e \rightarrow B^8\text{-}n\text{-pentyl}^{\bullet -} \quad (16)$$

$$B^8 - n - \text{pentyl} - e \rightarrow B^8 - n - \text{pentyl}^{\bullet +} \quad (17)$$

$$B^8\text{-}n\text{-pentyl}^{\bullet -} + B^8\text{-}n\text{-pentyl}^{\bullet +} \rightarrow (B^8\text{-}n\text{-pentyl}^{+}B^8\text{-}n\text{-pentyl}^{-})^{*} \text{ (excited aggregate formation)} \quad (18)$$

$$B^8\text{-}n\text{-pentyl}^{\bullet -} + B^8\text{-}n\text{-pentyl}^{\bullet +} \rightarrow {}^1B^8\text{-}n\text{-pentyl}^{*} + B^8\text{-}n\text{-pentyl} \quad (19)$$

$$(B^8\text{-}n\text{-pentyl}^{+}B^8\text{-}n\text{-pentyl}^{-})^{*} \rightarrow (B^8\text{-}n\text{-pentyl}^{+}B^8\text{-}n\text{-pentyl}^{-}) + h\nu \quad (20)$$

A degree of aggregation of 2 is shown in the proposed mechanism, but a higher degree of aggregation is also possible.

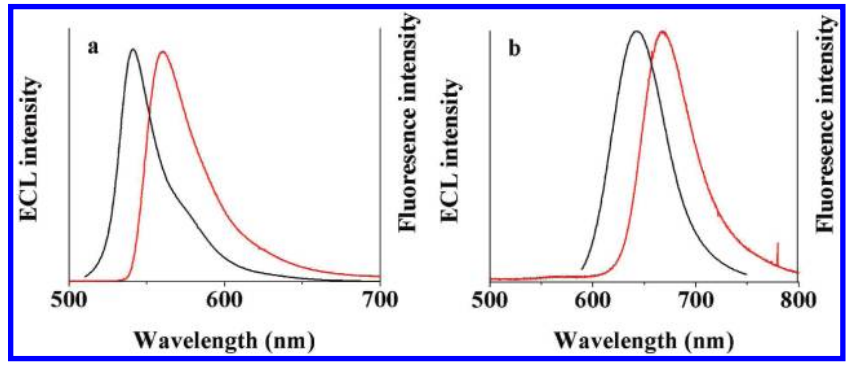

Figure 8. (a) ECL (red line) for 1 mM and fluorescence spectra for 2 μM B^8-phenyl in DCM. ECL spectra were generated by a pulsing potential at a frequency of 10 Hz from 1.09 to −1.48 V. (b) Same studies for the dimer except that the potential was stepped from 1.05 to −1.42 V. Platinum electrode area = 0.0314 cm^2; 0.1 M $TBAPF_6$ was used as a supporting electrolyte for all measurements. Stepping time, 1 min.

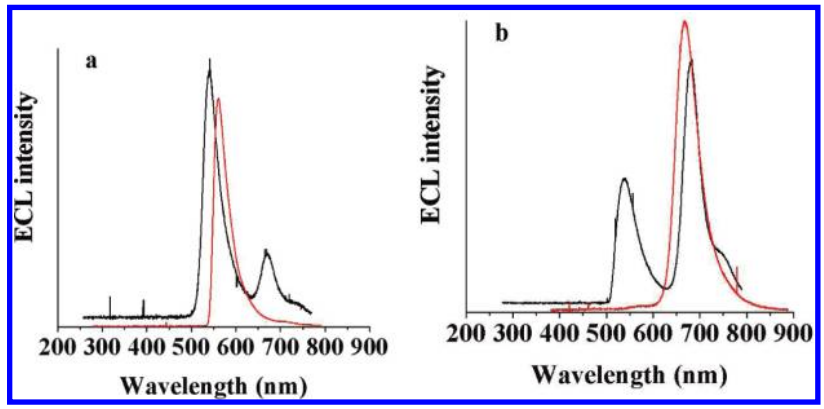

Figure 9. ECL results for the comparison of ECL for (a) 0.2 mM B^8-*n*-pentyl (black line) in acetonitrile and B^8-phenyl (red line) in DCM. The black line was multiplied by five. (b) 1 mM B^8-*n*-pentyl in acetonitrile (black line) and the dimer in DCM (red line). ECL was generated while pulsing the 0.0314 cm^2 platinum electrode with a frequency of 10 Hz from for B^8-*n*-pentyl, B^8-phenyl, and the dimer. Pulsing potentials are from −1.29 to 1.38 V for B^8-*n*-pentyl, 1.09 to −1.48 V for B^8-phenyl, and 1.05 to −1.42 V for the dimer; 0.1 M $TBAPF_6$ was used as a supporting electrolyte for all measurements. Stepping time, 1 min.

The main feature of an aggregate with a long-wavelength emission close to that of the covalent dimer with a perpendicular orientation is seen in this case (Figure 9).[27]

Perhaps the presence of the *n*-pentyl chain assists in the formation of the aggregates because an analogous process is not seen with the phenyl substituent. The possibility of forming excimers or aggregates for the BODIPY compounds with a long chain present has already been shown in the case of lipid systems where long-wavelength red fluorescence at 630 nm corresponding to the main fluorescence peak at 515 nm is observed.[32,33] The formation of aggregates with long-wavelength emission close to that seen for the covalent dimer has also been reported in a frozen matrix at low temperatures for a BODIPY dye.[27] However, we did not observe any difference in a DCM matrix of fluorescence at 77 K and at room temperature for B^8-*n*-pentyl (Supporting Information Figure S4). The ECL technique can provide some insight into intermolecular interactions that describe some degree of bonding that is not obtained by CV, but a clear identification of the products remains challenging.

5. Conclusions

ECL annihilation studies of B^8-*n*-pentyl dye radical ions show the presence of long-wavelength emission (in addition to the short-wavelength emission seen in photoluminescence). This is ascribed to the formation of aggregates during the annihilation. ECL spectra generated by only reduction or oxidation in the presence of co-reactant show the absence of the longer-wavelength emission. The presence of an alkyl chain can cause interactions between BODIPY monomers that assist in aggregate formation. Cyclic voltammetry studies of the aromatic dimer show the presence of two separate peaks, which is seen as evidence of a high degree of structural conjugation for the covalent dimers. B^8-phenyl did not aggregate, probably because of the absence of any long or short alkyl chains. Both compounds show CV characteristic for compounds that are completely substituted with alkyl and aryl groups with electrochemically reversible one-electron reduction and oxidation and one ECL maximum at a wavelength close to the fluorescence wavelength.

Acknowledgment. We thank the Center for Electrochemistry, Roche, Inc., and the Robert A. Welch Foundation (F-0021) for the support of this research and Craig Cone for assistance with low-temperature fluorescence measurements.

Supporting Information Available: Additional experimental results. This material is available free of charge via the Internet at http://pubs.acs.org.

References and Notes

(1) Loudet, A.; Burgess, K. *Chem. Rev.* **2007**, *107*, 4891–4932, and references therein.
(2) Rousseau, T.; Cravino, A.; Bura, T.; Ulrich, G.; Ziessel, R.; Roncali, J. *Chem. Commun.* **2009**, 1673–1675.
(3) Bouit, P. A.; Kamada, K.; Feneyrou, P.; Berginc, G.; Toupet, L.; Maury, O.; Andraud, C. *Adv. Mater.* **2009**, *21*, 1151–1154.
(4) Golovkova, T. A.; Kozlov, D. V.; Neckers, D. C. *J. Org. Chem.* **2005**, *70*, 5545–5549.
(5) Urano, Y.; Asanuma, D.; Hama, Y.; Koyama, Y.; Barrett, T.; Kamiya, M.; Nagano, T.; Watanabe, T.; Hasegawa, A.; Choyke, P. L.; Kobayashi, H. *Nat. Med.* **2009**, *15*, 104–109.
(6) Gabe, Y.; Urano, Y.; Kikuchi, K.; Kojima, H.; Nagano, T. *J. Am. Chem. Soc.* **2004**, *126*, 3357–3367.
(7) Ueno, T.; Urano, Y.; Kojima, H.; Nagano, T. *J. Am. Chem. Soc.* **2006**, *128*, 10640–10641.
(8) Lee, H. Y.; Bae, D. R.; Park, J. C.; Song, H.; Han, W. S.; Jung, J. H. *Angew. Chem., Int. Ed.* **2009**, *48*, 1239–1243.
(9) Lai, R. Y.; Bard, A. J. *J. Phys. Chem. B* **2003**, *107*, 5036–5042.
(10) Sartin, M. A.; Camerel, F.; Ziessel, R.; Bard, A. J. *J. Phys. Chem. C* **2008**, *112*, 10833–10841.
(11) Nepomnyashchii, A. B.; Bard, A. J. Unpublished results.
(12) Kollmannsberger, M.; Garies, T.; Heinl, S.; Breu, J.; Daub, J. *Angew. Chem., Int. Ed.* **1997**, *36*, 1333–1335.
(13) Trieflinger, C.; Röhr, H.; Rurack, K.; Daub, J. *Angew. Chem., Int. Ed.* **2005**, *44*, 6943–6947.
(14) Röhr, H.; Trieflinger, C.; Rurack, K.; Daub, J. *Chem.—Eur. J.* **2006**, *12*, 689–700.
(15) (a) *Electrogenerated Chemiluminescence*; Bard, A. J., Ed.; Marcel Dekker; New York, 2004. (b) Richter, M. *Chem. Rev.* **2004**, *104*, 3003–3036. (c) Miao, W. *Chem. Rev.* **2008**, *108*, 2506–2553.
(16) Leland, J. K.; Powell, M. J. *J. Electrochem. Soc.* **1990**, *137*, 3127–3131.
(17) Miao, W.; Choi, J. P.; Bard, A. J. *J. Am. Chem. Soc.* **2002**, *124*, 14478–14485.
(18) White, H. S.; Bard, A. J. *J. Am. Chem. Soc.* **1982**, *104*, 6891–6895.
(19) Chandross, E. A.; Sonntag, F. I. *J. Am. Chem. Soc.* **1966**, *88*, 1089–1096.
(20) Akins, D. L.; Birke, R. L. *Chem. Phys. Lett.* **1974**, *29*, 428–435.
(21) Santa-Cruz, T. D.; Akins, D. L.; Birke, R. L. *J. Am. Chem. Soc.* **1976**, *98*, 1677–1682.
(22) Bröring, M.; Krüger, R.; Link, S.; Kleeberg, C.; Köhler, S.; Xie, X.; Ventura, B.; Flamigni, L. *Chem.—Eur. J.* **2008**, *14*, 2976–2983.
(23) Rudolph, M. *J. Electroanal. Chem.* **1991**, *314*, 13–22.
(24) Rudolph, M. *J. Electroanal. Chem.* **1992**, *338*, 85–98.

(25) Mocak, J.; Feldberg, S. W. *J. Electroanal. Chem.* **1997**, *378*, 31–37.

(26) Feldberg, S. W.; Goldstein, C. I.; Rudolph, M. *J. Electroanal. Chem.* **1996**, *413*, 25–36.

(27) Ventura, B.; Marconi, G.; Bröring, M.; Krüger, R.; Flamigni, L. *New J. Chem.* **2009**, *33*, 428–438.

(28) Nepomnyashchii, A. B.; Cho, S.; Rossky, P. J.; Bard, A. J. To be published.

(29) Choi, J.-P.; Wong, K.-T.; Chen, Y.-M.; Yu, J.-K.; Chou, P.-T.; Bard, A. J. *J. Phys. Chem. B* **2003**, *107*, 14407–14413.

(30) Zhang, D.; Wen, Y.; Xiao, Y.; Yu, G.; Liu, Y.; Qian, X. *Chem. Commun* **2008**, 4777–4779.

(31) Prieto, I.; Teetsov, J.; Fox, M. A.; Vanden Bout, D.; Bard, A. J. *J. Phys. Chem. A* **2001**, *105*, 520–523.

(32) Pagano, R. E.; Chen, C.-S. *Ann. N.Y. Acad. Sci.* **1998**, *845*, 152–160.

(33) Bergström, F.; Mikhaylov, I.; Hägglöf, P.; Wortmann, R.; Ny, T.; Johannson, L. B.-Å. *J. Am. Chem. Soc.* **2002**, *124*, 196–204.

JP105312J